

**Accurate measurement of Rn decay product concentration ratios for  
determining air exchange rate and Rn source in rooms**

R. Rolle

Isotope Laboratory, Institute of Physical Chemistry, University of Goettingen  
37077 Goettingen, Germany  
<rrolle@gwdg.de>

**MEASUREMENT RELEVANCE**

The lung cancer risk from the (potential) alpha emission of inhaled radon decay products is considered the main radiation burden of man. Mostly in situations of elevated potential alpha energy concentrations (PAEC – working level WL) mitigation can bring meaningful long-term exposure reduction. The exposure dynamics involve the rate constants of the -

- variability of the sources of  $^{222}\text{Rn}$  and  $^{220}\text{Rn}$  (+ external sources of decay products),
- decay of  $^{222}\text{Rn}$ ,  $^{218}\text{Po}$ ,  $^{214}\text{Pb}$ ,  $^{214}\text{Bi}$ ,  $^{220}\text{Rn}$ , ( $^{216}\text{Po}$ ),  $^{212}\text{Pb}$ ,  $^{212}\text{Bi}$   
at  $t_{1/2}$ : 3.8d, 3min, 27min, 20min      56s, ( $1/7\text{s}$ ), 10.6h, 60min
- attachment of the decay product unattached clusters to aerosol (@ size distribution),
- room air exchange (variable - 0.1 to 10 air changes per hour),
- inhalation rate and retention in the lung,
- lung clearance rates of retained decay products.

When attempting to relate measurements to relevant exposure conditions more detailed information can be most useful and cost saving near or above prescribed action levels, particularly for more critical or problematic mitigation decisions.

The lung concentrates the decay products continuously and this can be more realistically simulated by concentrating and differentiating the individual decay products for measurement, rather than by a sometimes poorly related gas measurement. When continuously concentrating at a flow-rate  $f$  and efficiency  $e_f$  a radionuclide with decay constant  $\ln 2/t_{1/2}$ , then the concentrated activity in the sample is equivalent to the activity in an effective source volume of air -  $ESV = f \cdot e_f \cdot t_{1/2} \cdot 1.44$ . For breathing rates and at a conventional sampling rate of e.g.  $f=2\ell \cdot \text{min}^{-1}$ , this  $ESV$ , for the five decay products listed above, is far greater than the detection volume of a non-concentrating gas monitor or the lung. Thus the sensitivity for continuous decay product measurement is usually far greater than for gas measurement. In decay product measurement, as for the lung, the sensitivity for  $^{216}\text{Po}$ , due to the short  $t_{1/2}=1/7\text{ s}$ , is insignificant, while in gas measurement  $^{216}\text{Po}$  within a second is in equilibrium with  $^{222}\text{Rn}$  and usually has the equivalent gas monitor detection volume.

A measurement is complete only when the measurement uncertainty is available. For interdependent species the covariance matrix is required and allows uncertainty calculation of

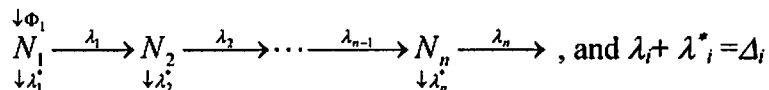
derived values. Good calibration is a prerequisite to obtain accurate results. Few available measurement systems fulfil the needs for critical mitigation decisions and an attempt is made below to indicate a way to better measurement.

### FLOW STRING EVALUATION

The vast majority of 'PAEC' measurements are made with long-term integrating passive Rn gas detectors and charcoal <sup>222</sup>Rn samplers, providing only a very coarse estimate of PAEC exposures. From PAEC exposures of the individual decay products, split into (two or more) aerosol size ranges, more realistic internal doses can be assessed. Conventionally with electronic instruments only an approximated, combined PEAC external exposure is measured. In some of the earliest methods of Rn decay product measurement for electronic instruments only a single gross alpha measurement (SGAM) was converted to PAEC. With current technology raw βα spectral data, measured online, while concentrating decay products on a screen (or several screens) and a filter, can readily be logged, together with ancillary data, at short intervals with small portable equipment. The (offline) computational evaluation of this data, provides optimal differentiation of varying individual decay product PAE concentrations or exposures, and associated covariance matrix. Subordinate to this self-evident system, and not necessarily ranking above optimised SGAM, lie any number of systems *cum* methods that use practically comparable electronic instrumentation and computational power, yet deliver far inferior exposure information and rarely provide statistical uncertainty.

The calculations involved in assessing sources, sinks and exposure situations are readily set up from string equations for flow (or decay) systems as follows:

For a constant source  $\Phi_1$  (e.g. flux in atoms.s<sup>-1</sup>) to a single string with branching(\*) flow/decay –



– all string members at equilibrium (observation time  $t \gg t_{1/2}$  of all string members) have –

$$\frac{\lambda_n N_n}{\Phi_{1,t \rightarrow \infty}} = \frac{\lambda_1}{\Lambda_1} \times \frac{\lambda_2}{\Lambda_2} \times \dots \times \frac{\lambda_n}{\Lambda_n} = \prod_{i=1}^n \frac{\lambda_i}{\Lambda_i} \quad (\text{for a non-branching string } \lambda_i = \Lambda_i \text{ :- } \frac{\lambda_n N_n}{\Phi_{1,t \rightarrow \infty}} = 1)$$

In a single tunnel the ventilation may be regarded as plug flow with negligible mixing across plug boundaries and the concentrations in a plug are described without ventilation-branching strings. In a room the air can be approximated as a well-mixed plug with ventilation (and surface plate-out) branches.

Non-equilibrium string flows  $N_i \lambda_i$  for a steady flux  $\Phi_1$  starting at  $t=0$  when all  $N_{i,t=0} = 0$  are given by:

$$\frac{\lambda_n N_{n,t}}{\Phi_{1,0 \rightarrow t}} = \left( \prod_{i=1}^n \frac{\lambda_i}{\Lambda_i} \right) - \sum_{i=1}^n \frac{e^{-\Lambda_i t}}{\Lambda_i} \prod_{j=1}^n \frac{\lambda_j}{\Lambda_j - \Lambda_i + \delta_{i,j}} \quad \dots (\delta_{i,j} = 1 \text{ for } i=j, \delta_{i,j} = 0 \text{ for } i \neq j),$$

while in the absence of a flux and  $N_{i>1,t=0} = 0$  :

$$\frac{\lambda_n N_{n,t}}{\lambda_1 N_{1,t=0}} = \frac{1}{\lambda_1} \sum_{i=1}^n e^{-\lambda_i t} \prod_{j=1}^n \frac{\lambda_j}{\Lambda_j - \Lambda_i + \delta_{i,j}}$$

The **response**, i.e. the integral flow or decays along the string, of member  $n$  over a period  $t_a \rightarrow t_b$  for a constant flux  $\Phi_1$  from  $t = 0$  to  $t_b$ , starting with  $N_{i \leq n} = 0$  at  $t = 0$ , is :

$$\frac{\int_0^{t_b} N_{n,t} \lambda_n dt}{\Phi_{1,t=0 \rightarrow t_b}} = \left( \frac{t_a - t_b}{\lambda_1} \prod_{i=1}^n \frac{\lambda_i}{\Lambda_i} \right) - \frac{1}{\lambda_1} \sum_{i=1}^n \frac{e^{-\lambda_i t_b} - e^{-\lambda_i t_a}}{-\Lambda_i^2} \prod_{j=1}^n \frac{\lambda_j}{\Lambda_j - \Lambda_i + \delta_{i,j}},$$

while the **response** of member  $n$  after terminating the flux at  $t_b$  during time  $t_c$  to  $t_d$  is:

$$\frac{\int_{t_c}^{t_d} N_{n,t} \lambda_n dt}{\Phi_{1,t=0 \rightarrow t_b}} = \sum_{k=1}^n \left\{ \left( \prod_{i=1}^k \frac{\lambda_i}{\Lambda_i} \right) - \sum_{i=1}^k \frac{e^{-\lambda_i t_b}}{\Lambda_i} \prod_{j=1}^k \frac{\lambda_j}{\Lambda_j - \Lambda_i + \delta_{i,j}} \right\} \left\{ \frac{1}{\lambda_k} \sum_{i=k}^n \frac{e^{-\lambda_i t_d - t_b} - e^{-\lambda_i t_c - t_b}}{-\Lambda_i} \prod_{j=k}^n \frac{\lambda_j}{\Lambda_j - \Lambda_i + \delta_{i,j}} \right\}.$$

The above equations can, with stepwise time shifts, be cumulatively applied to step changes in source fluxes and rate constants, and can thus, at adequately short time steps accommodate arbitrary progressions. For a network of flows the individual string responses, divided by their  $\lambda_i$  to derive the  $N_i$ , are summed at the nodes and weighted proportionally for duplication of common leading string sections. A measured response, that is the counts  $N_i$  in a particular spectral regions of interest (ROI) and counting interval is related, by the (large number of) above string calculations to all the relevant foregoing flux steps.

Shown in Fig. 1. is a simplified flow- or string scheme indicating relevant parameters in a Rn (single) source 'room'. For consecutive rooms or with significant Rn and decay product activity in the air intake, the decay product sources also need to be taken account of. They can usually be measured independently at the transition location. For a measurable activity space profile in a room the room can be evaluated as separate compartments.

Typically data from a continuous room measurement need to be evaluated as follows. A data set is obtained from sampling  $^{218}\text{Po}$ ,  $^{214}\text{Pb}$  and  $^{214}\text{Bi}$  concentrations continuously and recording spectral data, over a time period where these concentrations possibly vary significantly, i.e. the fluxes  $\Phi_{i,t}$  (onto a filter) vary with time. A plot of the 6 MeV spectral peak window, i.e. ROI counts, vs. time will indicate the time steps over which the concentrations should be separately evaluated; alternately regular short concentration intervals could be chosen. For presumably non-changing concentrations the data could be evaluated for only a single concentration step as in batch-, or grab-sampling measurement. In the evaluation of the data, every individually recorded (ROI) count  $N$  is related, via filtration rate and efficiency, detection efficiency in ROI and either of the last two response equations above, by a factor  $k$  to all the individual activity concentrations in every concentration [  $j$  ] time step up to the end of that count:

$$N_i + \epsilon_i = k_{i,1} \times [^{218}\text{Po}_1] + k_{i,2} \times [^{218}\text{Po}_2] + \dots + k_{i,20} \times [^{214}\text{Pb}_1] + k_{i,21} \times [^{214}\text{Pb}_2] + \dots + k_{i,30} \times [^{214}\text{Bi}_1] + \dots \\ = \sum_j k_{ij} \times C_j,$$

(with possible additional components  $j$ , such as background ( $^{210}\text{Po}$ ) count rate,  $^{212}\text{Pb}$  and  $^{212}\text{Bi}$  concentrations). A weighted least squares calculation of all available  $N_i$  equations yields the

individual concentrations for all the time steps, and the appropriate uncertainty evaluation yields the covariance matrix. Other parameters, such as PAE concentrations, can then be derived from these results.

### OBSERVATIONS ON MEASUREMENTS AND SYSTEMS

In Fig. 2 the strong concentration dependence on air exchange rate of  $^{222}\text{Rn}$  and the lung-exposure-relevant decay products for a room with a flux from a 10 kBq (emanating)  $^{226}\text{Ra}$  and a 10kBq  $^{224}\text{Ra}$  source.vol<sup>-1</sup> is shown. In Fig. 3, for the same air exchange range, the (potential alpha energy) equilibrium factor F for  $^{222}\text{Rn}$  is shown, as well as the activity ratios of  $^{218}\text{Po}/^{222}\text{Rn}$  and  $^{214}\text{Bi}/^{218}\text{Po}$ . Estimation of PAE from a measurement of  $^{222}\text{Rn}$  gas and a presumed F factor is thus coupled with a substantial (systematic) uncertainty range at unknown air exchange rate. The indicated measurement of individual Rn decay product concentrations, using almost comparable electronic instrumentation to gas measurement, does not include this uncertainty for PAE, and since the effective source volume is far greater than for gas measurement, the statistical uncertainty is also far better than in gas measurement. Conversely, for the calculation of  $^{222}\text{Rn}$  concentration from individual decay product measurements, for instance the two decay product ratio curves in Fig. 3 show that the air exchange rate can readily be assessed from the measured  $^{214}\text{Bi}/^{218}\text{Po}$  ratio. The  $^{222}\text{Rn}$  concentration is then obtained via the  $^{218}\text{Po}$  concentration at this exchange rate – probably at better accuracy than direct gas measurement.

The simplified example above can be extended, with more appropriate calculation and extension of the string model, to the evaluation of the effective  $^{226}\text{Ra}$  source(s) and air exchange rates and their time dependence in various environments. Using e.g. an inline screen and filter instrument, the individual unattached and attached Rn decay product concentrations can be measured and the attachment time-constants can be determined. Having assessed prevailing sources of Rn and ventilation, and their time dependence, then the string calculations indicated above can be used to model the effect of various choices of mitigation measures, and to choose the most cost effective ones, and in stepwise implementation to verify their effectiveness. Mere Rn concentration measurement would allow only far less objective mitigation.

In the  $\alpha$  determination of Pb and Bi concentrations simultaneously, both are measured via the same  $\alpha$  emissions of Po and differentiation of the two concentrations is only feasible on the basis of their sequential buildup and decay behaviour. With the halflife of Bi shorter than that of Pb, when differentiating them by sequential  $\alpha$ -measurement, the statistical precision of a determination is seriously impaired. With current technology of Si-detectors and signal amplification stable  $\beta$ -measurement can readily be included in the conventional  $\alpha$ -spectrometric measurement, improving the differentiation of individual decay product concentrations about tenfold (Rolle and Lettner, 1998). When significant concentrations of only  $^{218}\text{Po}$ ,  $^{214}\text{Pb}$  and  $^{214}\text{Bi}$  are present, then measurement by  $\beta\alpha$ -spectrometry offers good differentiation of these, even without the sequential buildup-decay manipulation of a measurement procedure, i.e. evaluation of 3 unknowns from 3 ROIs (partially overlapping). Time sequences of the three concentrations could be evaluated from continuously sampled and sequentially recorded  $\beta\alpha$ -spectra/ROIs. When in addition also significant concentrations of  $^{212}\text{Pb}$  and  $^{212}\text{Bi}$  are present, then essentially

only 4 spectral  $\beta\alpha$ -ROIs are available for the 5 concentrations. Here quasi-continuous sampling (½h on, ½h off) with sequential recording of  $\beta\alpha$ -spectral data is a good choice for many applications.

## CALIBRATION OF RADON DECAY PRODUCT MONITORS

A measurement is no better than the underlying calibration permits.

Conventional calibration for Rn decay product concentration measurement may have sufficed in the past for the applications used, but would not meet the accuracy requirements for the more demanding measurement applications proposed here.

Airflow can normally be adequately controlled within a few percent while the aerosol retention efficiency for prescribed filters usually exceeds 99%. Conventional  $\alpha$ -detection efficiency calibration was normally carried out using a metal disc with a thinly plated, long-lived  $\alpha$ -emitter of certified activity and matching active diameter. In a few instances  $^{214}\text{Pb}$  and  $^{214}\text{Bi}$  activities on measurement filters (and screens) were measured in both the monitor and by  $\gamma$ -spectrometry (traceable to national standards).

For an optimised filter and detector combination the  $\alpha$  spectrum shows substantial, variable spectrometric peak tailing. This results from energy loss of the emitted  $\alpha$ -particles from the collected activity to the active volume of the detector – roughly  $\frac{1}{3}$  each in the filter, the airgap and the detector window. The aerosol particles partly penetrate the filter to depths that, in continuous sampling, change with filter loading and aerosol consistency, thus modifying the tailing and relative detection efficiency in adjacent spectrometric ROIs. This behaviour cannot be accommodated with conventional fixed calibration factors.

An accurate  $\alpha$ -calibration for filter and detector geometry has been developed, based on analytical calculation of fractional solid angles for every sample element, as shown in Fig. 4, and residual energy calculation in penetrating successive layers of filter, air and detector window. Adjusting an initially unknown exponential depth distribution parameter for optimal fit to measured spectral profiles provides the per channel or ROI detection efficiency for each emitted  $\alpha$ -energy calculated. Spectral tail shape matching over 4 decades of intensity has substantiated the correctness of the computation. The  $\alpha$ -absorption curves for different materials are available from a SRIM package (the Stopping and Range of Ions in Matter - Ziegler *et al.* 1985/2000). This calibration has been extensively used for measurement data sets with presumed non-changing spectral tail shapes – incorporation with automated shape matching into the evaluation of continuously recorded spectral data with progressive ‘filter loading’ is the next step.

The  $\beta$ -detection efficiencies, in a common ROI above a 100keV threshold, for Rn-decay products on a filter have to date been derived in measurement sequences where the  $\alpha$ -calibration and  $\alpha$ -activities have been accurately determined. Experience with the computational  $\alpha$ -

calibration has provided inspiration to proceed also with the computation of  $\beta$ -detection efficiencies, excluding the energy region below 100keV.

To date for wire mesh screens, used for aerosol size-differentiating measurement, the  $\beta$ - and  $\alpha$ -detection efficiencies for  $^{214}\text{Pb}$  and  $^{214}\text{Bi}$  have been scaled from filter detection efficiencies (or  $\gamma$ -measurement). The ventilation applications outlined in this paper point out the need also for more accurate calibration for screens. The considerably more cumbersome computation of detector-subtended, solid angles for all the surface elements of a woven wire screen cell is in progress. Additional impetus for this task has come from a very similar need, i.e. to determine the recoil loss factor for screen collected  $^{218}\text{Po}$  that  $\alpha$ -recoil on decay to  $^{214}\text{Pb}$ . The neglect of this factor has resulted in underestimating the concentration of unattached  $^{214}\text{Pb}$ , a species with enhanced lung deposition.

### CONCLUSIONS

Important metrology applications in Rn radiation protection are locating 'buildings' with (potentially) high indoor (Rn) Rn decay product levels and making proper mitigating decisions. A major application requires cost-effective screening measurements of adequate PAEC precision. Another is in critical situations with a need, instead of mere  $^{222}\text{Rn}$  level measurement, for cost-effective determination of Rn sources and air exchange rate, evaluated via room modelling with input of decay product measurements of enhanced accuracy. Subsequently mitigating options can be modelled more objectively for the most cost-effective reduction of concentrations, and can be re-evaluated after (stepwise) mitigation. The instrumental requisites for this decay product measurement are only marginally above those of commercially available active monitors for Rn and/or decay products, and have been implemented on a batch of instruments. A software package for concentration evaluation of the sequentially logged spectral data has been developed, as well as a program for accurate  $\alpha$ -calibration of filters. Forthcoming software will extend the enhanced accuracy calibration to screens and for  $\beta$ -calibration. Beyond this, a range of software to simplify the more elaborate combination of strings for system evaluation is foreseen.

REFERENCES

R. Rolle and H. Lettner: 'An analysis of efficient measurement procedures for radon progeny.' Environment International, Vol. 22 Suppl. 1, pp. S585-S593, 1996.

Ziegler, J. F., Biersack, J.P., Littmark, U., 1985. The Stopping and Range of Ions in Solids, Pergamon Press, New York.

Figures – Note to editor: - (The figure titles of figures 2 - 4 are in separate, transparent text boxes). Figures 2 and 3 are screen copy-and-paste from an APL+win application. Please email <rrolle@gwdg> if better resolution or different type size is required. Figure 4 is also available in the attached Powerpoint File – renoppt2.ppt

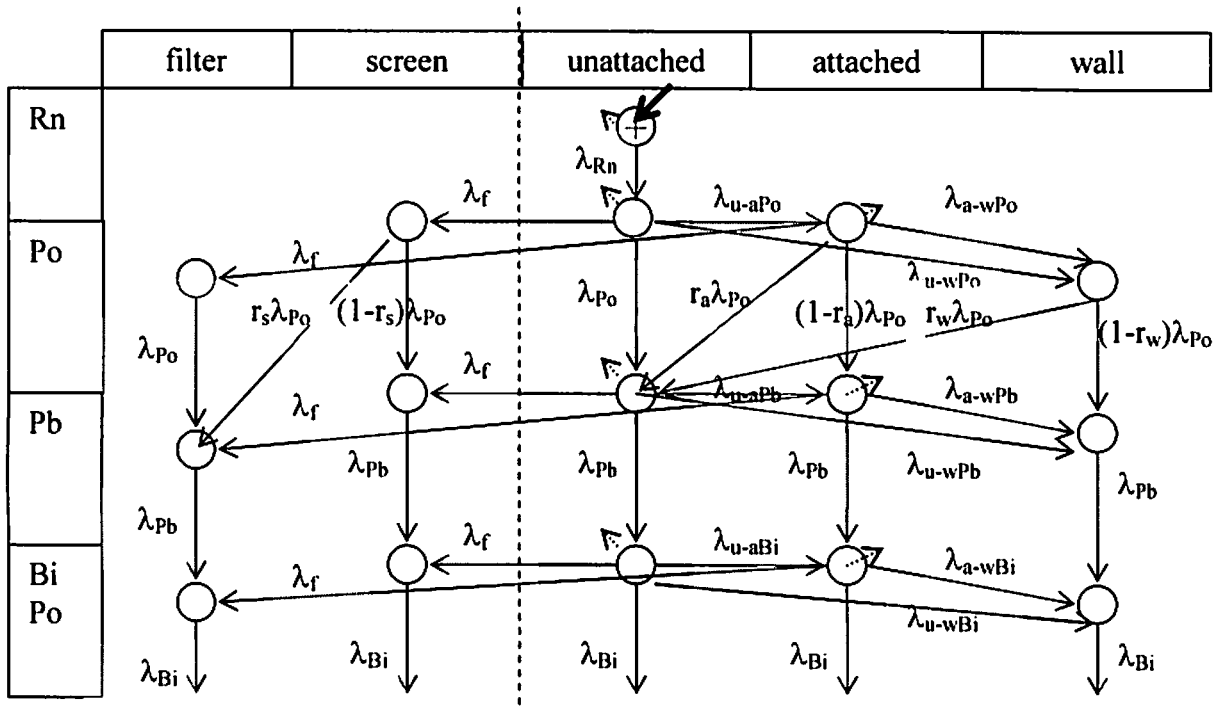


Figure 1. Simple model string (flow) scheme showing transformation rate constants effective in a room with a Rn source and air exchange (short arrows);  $\lambda_{u-a}$  - attachment rate to aerosol,  $\lambda_{u-w}$  to wall;  $r_a$ ,  $r_w$  – recoil fractions. The sampling or 'breathing' section (left of dotted line) can normally be treated independently, and the wall section would normally be considered a refinement.

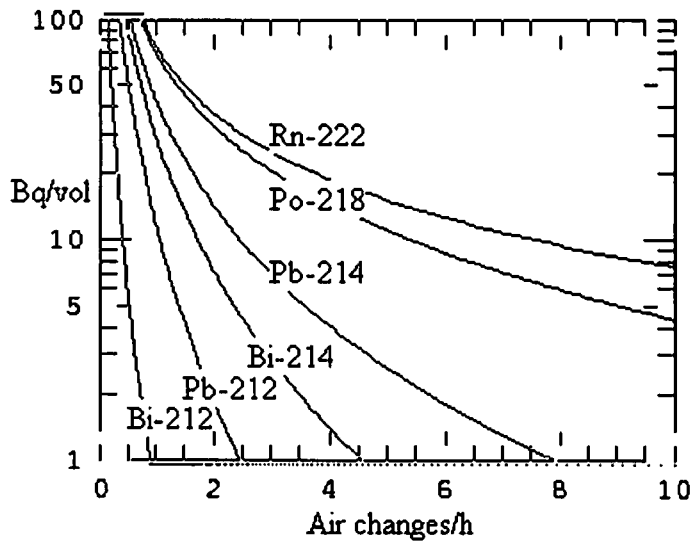


Fig. 2. Effect of air exchange rate at a  $^{222}\text{Rn}$  and  $^{220}\text{Rn}$  flux from  $10\text{kBq } ^{226}\text{Ra}$  and  $10\text{kBq } ^{228}\text{Ra}$  into a volume.

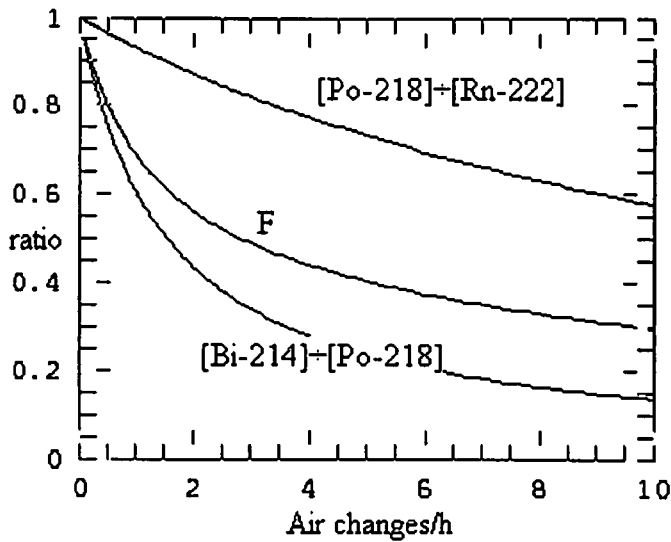


Figure 3. Effect of air exchange rate in a room on the Rn PAE equilibrium factor  $F$ , and on activity ratios of  $^{222}\text{Rn}$ ,  $^{218}\text{Po}$  and  $^{214}\text{Bi}$ .



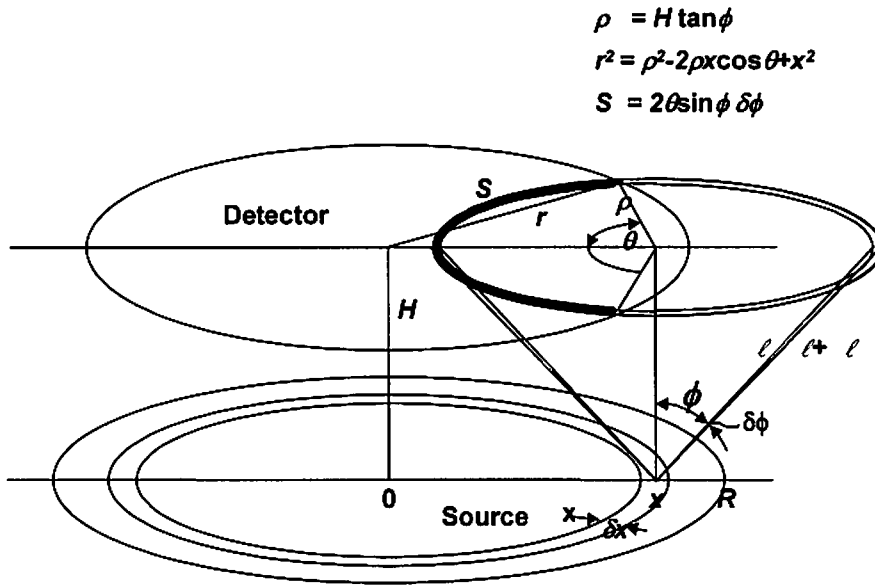


Figure 4. Solid angle and absorption path for calculation of  $\alpha$  detection efficiencies.